HIGH ENERGY pp COLLISIONS IN ADDITIVE QUARK MODEL

Yu.M. Shabelski and A.G. Shuvaev
[arXiv:1504.03499]
Petersburg Nuclear Physics Institute, Kurchatov National Research Center
Gatchina, St. Petersburg 188300, Russia

High energy (CERN SPS and LHC) pp ($p\bar{p}$) scattering is treated in the framework of Additive Quark Model (AQM) together with Pomeron exchange theory. In AQM baryon is treated as a system of three colored constituent quarks having internal quark-gluon structure and finite radius, $r_q^2 \ll r_p^2$, where r_p is proton radius. The amplitude of constituent quarks scattering is given by one-Pomeron exchange,

$$M_{qq}^{(1)}(s,t) = \gamma_{qq}(t) \cdot \left(\frac{s}{s_0}\right)^{\alpha_P(t)-1} \cdot \eta_P(t), \qquad \eta_P(t) \,=\, i \,-\, \tan^{-1}\left(\frac{\pi\alpha_P(t)}{2}\right),$$

with the Pomeron trajectory $\alpha_P(t) = \alpha_P(0) + \alpha'_P \cdot t$ specified by the intercept, $\alpha_P(0)$, and slope, α'_P, values. $\gamma_{qq}(t) = g_1(t) \cdot g_2(t)$ is the Pomeron coupling to the beam and target particles, $g_{1,2}(t)$ are the vertices of constituent quark-Pomeron interaction.

The elastic pp ($p\bar{p}$) scattering amplitude is expressed through the initial, $\psi(k_i)$, and final, $\psi(k_i + Q_i)$, proton wavefunctions written in terms of the constituent quarks' momenta k_i,

$$M_{pp}(s,t) \,=\, \int dK\, dK' \psi^*(k'_i + Q'_i)\, \psi^*(k_i + Q_i)\, V(Q,Q')\, \psi(k'_i)\, \psi(k_i),$$

$$dK \,\equiv\, d^2k_1 d^2k_2 d^2k_3\, \delta^{(2)}(k_1 + k_2 + k_3), \quad \psi(k_i) \equiv \psi(k_1, k_2, k_3).$$

The interaction vertex $V(Q,Q') \equiv V(Q_1,Q_2,Q_3,Q'_1,Q'_2,Q'_3)$ stands for the multipomeron exchange, Q_k and Q'_l are the momenta transferred to the target quark k or beam quark l by the Pomerons attached to them, Q is the total momentum transferred in the scattering, $Q^2 = -t$.

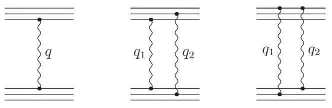

Several AQM diagrams for pp elastic scattering. The straight lines stand for quarks, the waved lines denote Pomerons. Diagram (a) is the one of the single Pomeron diagrams, diagrams (b) and (c) represent double Pomeron exchange with two Pomeron coupled to the different quark (b) and to the same quarks (c), $q_1 + q_2 = Q$.

The scattering amplitude is presented in AQM as a sum over the terms with a given number of Pomerons,

$$M_{pp}(s,t) \,=\, \sum_n M_{pp}^{(n)}(s,t),$$

where the amplitudes $M_{pp}^{(n)}$ collect all diagrams comprising various connections of the beam and target quark lines with n Pomerons.
AQM permits the Pomeron to connect any two quark lines only once. It crucially decreases the combinatorics leaving the diagrams with no more than $n = 9$ effective Pomerons.

The Pomeron trajectory is assumed in the simplest form,

$$\left(\frac{s}{s_0}\right)^{\alpha_P(t)-1} = e^{\Delta\cdot\xi} e^{-r_q^2 q^2}, \quad \xi \equiv \ln\frac{s}{s_0}, \quad r_q^2 \equiv \alpha' \cdot \xi \;\; \text{radius of quark-quark interaction,} \qquad S_0 = (9\ \text{GeV})^2.$$

In the first order there are 9 equal quark-quark contributions due to one Pomeron exchange between qq pairs, $M_{pp}^{(1)} \,=\, 9\Big(\gamma_{qq}\eta_P(t)e^{\Delta\cdot\xi}\Big)\, e^{-r_q^2 Q^2} F_P(Q,0,0)^2$, expressed through the overlap function

$$F_P(Q_1,Q_2,Q_3) \,=\, \int dK\, \psi^*(k_1,k_2,k_3)\, \psi(k_1+Q_1, k_2+Q_2, k_3+Q_3).$$

The function $F_P(Q,0,0)$ plays a role of proton formfactor for the strong interaction in AQM.

Elastic scattering. The higher orders terms are expressed through the functions F_P integrated over Pomerons' momenta, $t_n \simeq t/n$,

$$M_{pp}^{(n)}(s,t) \,=\, i^{n-1}\Big(\gamma_{qq}\eta_P(t_n)e^{\Delta\cdot\xi}\Big)^n \int \frac{d^2q_1}{\pi}\cdots\frac{d^2q_n}{\pi}\,\pi\,\delta^{(2)}(q_1 + \ldots + q_n - Q)$$
$$\times\, e^{-r_q^2(q_1^2+\ldots+q_n^2)}\,\frac{1}{n!}\sum_{n\ \text{connections}} F_P(Q_1,Q_2,Q_3)\, F_P(Q'_1,Q'_2,Q'_3),$$

The sum refers to all distinct ways to connect the beam and target quark lines with n Pomerons.

The differential cross section in the normalization adopted here is evaluated as

$$\frac{d\sigma}{dt} \,=\, 4\pi\,|M_{pp}(s,t)|^2, \quad \sigma_{pp}^{tot} \,=\, 8\pi\,\mathrm{Im}\,M_{pp}(s,t=0)\ \text{optical theorem.}$$

Single and double diffractive dissociation.

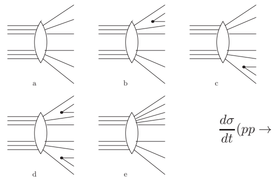

Different final states in the high energy pp collision: a) elastic pp scattering, b) and c) single diffractive dissociation of first or second proton, d) double diffractive dissociation, e) process with one $q\bar{q}$ pair inelastic production that does not contribute to the calculated σ_{SD} but can contribute to the experimental value σ_{SD}.

$$\frac{d\sigma}{dt}(pp \to p'p') = \frac{d\sigma}{dt}(pp \to pp) + 2\frac{d\sigma}{dt}(pp \to p^*p) + \frac{d\sigma}{dt}(pp \to p^*p^*)$$

The amplitude of single diffraction dissociation

$$M_{SD}(s,t) \,=\, \int dK\, dK' \psi^*(k'_i + Q')\, \tilde{\psi}_m^*(k_i + Q_i) \times V(Q,Q')\, \psi(k'_i)\, \psi(k_i).$$

The amplitude of double diffraction dissociation

$$M_{DD}(s,t) \,=\, \int dK\, dK' \tilde{\psi}_m^*(k'_i + Q')\, \tilde{\psi}_n^*(k_i + Q_i) \times V(Q,Q')\, \psi(k'_i)\, \psi(k_i)$$

To obtain cross section one has to square the module of an appropriate amplitude. Making no distinction between the individual final states it should be summed up over m for SD process or over m and n indices for DD process. Using the completeness condition,

$$\sum_n \tilde{\psi}_n(p_i + Q''_i)\, \tilde{\psi}_n^*(k_i + Q_i) \,=\, \delta^{(2)}(p_i + Q''_i - k_i - Q_i)$$

along with the same condition for the index m we get

$$\frac{d\sigma_{el}}{dt} + 2\,\frac{d\sigma_{SD}}{dt} + \frac{d\sigma_{DD}}{dt} = \sum_{m,n} |M_{p'p'}^{(m,n)}|^2(s,t)$$
$$|M_{p'p'}^{(m,n)}|^2 \,=\, \Big(\gamma_{qq}e^{\Delta\cdot\xi}\Big)^{m+n}\big[\,i\eta_P(t_m)\big]^m\big[-i\eta_P^*(t_n)\big]^n$$
$$\times \int \frac{d^2q_1}{\pi}\cdots\frac{d^2q_m}{\pi}\pi\,\delta^{(2)}(q_1 + \ldots + q_m - Q)$$
$$\times\, \frac{d^2q_{m+1}}{\pi}\cdots\frac{d^2q_{m+n}}{\pi}\,\pi\,\delta^{(2)}(q_{m+1} + \ldots + q_{m+n} - Q) \times e^{-r_q^2(q_1^2+\ldots+q_{m+n}^2)}$$
$$\times \frac{1}{m!}\,\frac{1}{n!}\sum_{m,n\ \text{connections}} F_P(Q_1,Q_2,Q_3)\, F_P(Q'_1,Q'_2,Q'_3).$$

$$\frac{d\sigma_{SD}}{dt} + \frac{d\sigma_{el}}{dt} = \sum_{m,n} |M_{pp'}^{(m,n)}|^2(s,t),$$
$$|M_{pp'}^{(m,n)}|^2 \,=\, \Big(\gamma_{qq}e^{\Delta\cdot\xi}\Big)^{m+n}\big[\,i\eta_P(t_m)\big]^m\big[-i\eta_P^*(t_n)\big]^n$$
$$\times \int \frac{d^2q_1}{\pi}\cdots\frac{d^2q_m}{\pi}\,\pi\,\delta^{(2)}(q_1 + \ldots + q_m - Q)$$
$$\times\, \frac{d^2q_{m+1}}{\pi}\cdots\frac{d^2q_{m+n}}{\pi}\,\pi\,\delta^{(2)}(q_{m+1} + \ldots + q_{m+n} - Q) \times e^{-r_q^2(q_1^2+\ldots+q_{m+n}^2)}$$
$$\times\, \frac{1}{m!}\frac{1}{n!}\sum_{m,n\ \text{connections}} F_P(Q_1,Q_2,Q_3) \times F_P(Q'_1,Q'_2,Q'_3)\ F_P(Q''_1,Q''_2,Q''_3)$$

Numerical results.

The overlap function F_P is evaluated through the transverse part of the quarks' wavefunction, which has been taken in a simple form of two gaussian packets,

$$\psi(k_1,k_2,k_3) \,=\, N\big[\,e^{-a_1(k_1^2+k_2^2+k_3^2)} \,+\, C\,e^{-a_2(k_1^2+k_2^2+k_3^2)}\big].$$

The Pomeron parameters are

$$\Delta = 0.107, \quad \alpha' = 0.31\,\text{GeV}^{-2}, \quad \gamma_{qq} = 0.44\,\text{GeV}^{-2},$$

and the parameters of matter distribution in the proton are

$$a_1 = 4.8\,\text{GeV}^{-2}, \quad a_2 = 1.02\,\text{GeV}^{-2}, \quad C = 0.133.$$

Note that the same set of the Pomeron parameters describes proton and antiproton scattering, therefore both pp and $p\bar{p}$ data have been commonly used to fix their values.

The model gives a reasonable description of elastic scattering experimental data both for pp collisions at $\sqrt{s} = 7$ TeV and $p\bar{p}$ collisions at $\sqrt{s} = 546$ GeV.

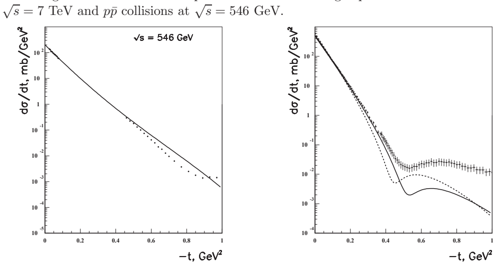

Figure 1: The differential cross section of elastic $p\bar{p}$ scattering at $\sqrt{s} = 546$ GeV (left panel) and for the elastic pp collisions at $\sqrt{s} = 7$ TeV (right panel, solid line) compared to the experimental data. The dotted line at the right panel shows the predicted elastic pp cross section at $\sqrt{s} = 13$ TeV. The experimental points have been taken from [4, 5, 6, 7].

The results for the SD and DD cross sections are presented in the Table.

$\sqrt{s}$	σ_{el} (mb)	$\sigma_{SD}(mb)$	$\sigma_{DD}(mb)$
546 GeV	14.3	2.3	2.6
7 TeV	27.3	4.3	3.9
13 TeV	31.6	5.4	4.9

The SD cross sections come out to be rather small, $\sigma_{SD}/\sigma_{el} \simeq 15 - 18\%$, that matches perhaps the experimental results at LHC energies [1, 2, 3]. The total diffraction cross section is approximately half the elastic one, $2\sigma_{SD} + \sigma_{DD} \simeq \sigma_{el}/2$, within the range of available energy dependence of the probability of diffractive to elastic scattering.

The ratio σ_{DD}/σ_{el} is not quadratically small compared to σ_{SD}/σ_{el}. The reason for this comes in AQM from an extra third formfactor F_P in the SD cross section (1) compared to the two formfactors in the DD formula. On the other hand the connection between diffractive cross section calculated in AQM and the experimental data is not straightforward since AQM comprises only a part of the processes involved in the scattering.

Motivated by the recently announced new LHC run we present also the predictions for the elastic pp scattering and diffractive dissociation at $\sqrt{s} = 13$ TeV. In particular, we expect the total cross section

$\sigma(pp)_{tot} = 110$ mb, the parameter of the elastic slope cone ($d\sigma/dt \sim \exp(-B \cdot t)$) $B = 21.8$ GeV^{-2}, the minimum position at $|t| = 0.45$ GeV^2 while our results for the differential cross section, $d\sigma_{el}/dt$, are shown in Fig. 1.

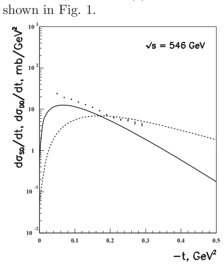

Figure 2: The cross section of single (solid line) and double (dotted line) diffractive dissociation in $p\bar{p}$ scattering at $\sqrt{s} = 546$ GeV. The experimental SD points have been taken from [8].

Fig. 2 shows our results for the differential cross sections $d\sigma_{SD}/dt$ and $d\sigma_{DD}/dt$ at $\sqrt{s} = 546$ GeV. The slope of the differential cross section at $|t| \simeq 0.2$ GeV^2 is $B_{SD} \simeq 10$ GeV^{-2} for the single diffractive diffraction and $B_{DD} \simeq 3$ GeV^{-2} for the double diffractive dissociation. These values are essentially smaller than the elastic slope that is about 15 GeV^{-2} [9].
Unfortunately we are unable to predict at small $|t| < 0.1$ Gev^2 because of the unknown effects of confinement that could lead to the transition between the ground and excited states. The region $|t| > 1$ Gev^2 is beyond the reach of our model as well since the internal structure of the constituent quarks can not be more ignored there. The diffractive cross section behavior in the intermediate interval is in reasonable agreement with the experimental data.

References

[1] G. Antchev *et al.* [TOTEM Collaboration], Europhys. Lett. **101** (2013) 21003.

[2] TOTEM coll. F. Oljemark and K. Osterberg "Studies of soft single diffraction with TOTEM at $\sqrt{s} = 7$ TeV" LHC students poster session, 13 March 2013.

[3] V. A. Khoze, A. D. Martin and M. G. Ryskin, Int. J. Mod. Phys. A **30** (2015) 08, 1542004, [arXiv:1402.2778 [hep-ph]].

[4] F. Abe *et al.* [CDF Collaboration], Phys. Rev. D **50** (1994) 5518.

[5] G. Antchev et al., TOTEM Collaboration, Europhys. Lett. **96**, 21002 (2011).

[6] TOTEM Collaboration, G. Antchev et al., Europhys.Lett. **101** (2013) 21002.

[7] TOTEM Collaboration, G. Antchev et al., Europhys.Lett. **95** (2011) 41001, [arXiv:1110.1385].

[8] D. Bernard *et al.* [UA4 Collaboration], Phys. Lett. B **186** (1987) 227.

[9] Y. M. Shabelski and A. G. Shuvaev, JHEP **1411** (2014) 023 [arXiv:1406.1421 [hep-ph]].